Development 140, 2050-2060 (2013) doi:10.1242/dev.087817

Laminins containing the β2 and γ3 chains regulate astrocyte migration and angiogenesis in the retina

Gopalan Gnanaguru, Galina Bachay, Saptarshi Biswas, Germán Pinzón-Duarte, Dale D. Hunter and William J. Brunken*

SUMMARY

Pathologies of retinal blood vessels are among the major causes of blindness worldwide. A key cell type that regulates retinal vascular development is the astrocyte. Generated extrinsically to the retina, astrocytes migrate into the retina through the optic nerve head. Even though there is a strong correlation between astrocyte distribution and retinal vascular development, the factors that guide astrocytes into the retina remain unclear. In this study, we show that astrocytes migrate within a laminin-containing basement membrane – the inner limiting membrane. Genetic deletion of the laminin β2 and γ3 chains affects astrocyte migration and spatial distribution. We show that laminins act as haptotactic factors *in vitro* in an isoform-specific manner, inducing astrocyte migration and promoting astrocyte differentiation. The addition of exogenous laminins to laminin-null retinal explants rescues astrocyte migration and spatial patterning. Furthermore, we show that the loss of laminins reduces β1 integrin expression in astrocytes. Culturing laminin-null retinal astrocytes on laminin substrates restores focal localization of β1 integrin. Finally, we show that laminins containing β2 and γ3 chains regulate subsequent retinal blood vessel growth and maintain vascular integrity. These *in vivo* and *in vitro* studies demonstrate clearly that laminins containing β2 and γ3 chains are indispensable for migration and spatial organization of astrocytes and that they play a crucial role during retinal angiogenesis *in vivo*.

KEY WORDS: Laminin, Integrins, Angiogenesis, Astrocyte, Retinopathy of prematurity, Mouse

INTRODUCTION

A thorough understanding of retinal vascular development is necessary because diseases of the retinal vasculature in either children (retinopathy of prematurity) or adults (diabetic retinopathy) are among the major causes of blindness (Chen and Smith, 2007; Sapieha et al., 2010; Kempen et al., 2004). During retinal angiogenesis, the retinal vasculature develops three interconnected capillary beds or layers: the superficial, intermediate and deep plexiform layers (Fruttiger, 2007). The first step in this development – the formation of the superficial layer – is wholly dependent on the presence of astrocytes. For example, vertebrate retinas that lack astrocytes never become vascularized; moreover, in humans and other primates, the fovea, which lacks astrocytes, remains avascular (Schnitzer, 1988; Provis and Hendrickson, 2008; Provis et al., 2000).

In vascularized retinas, astrocytes enter the retina through the optic nerve head (ONH) (Watanabe and Raff, 1988). Upon entry, astrocytes proliferate and spread across the entire surface of the retina in a centrifugal fashion, in part directed by retinal ganglion cells (Fruttiger et al., 1996; Fruttiger et al., 2000; Fruttiger, 2007). During their migration to the periphery, astrocytes serve as a template for endothelial cells to follow, thereby guiding the formation of the superficial vasculature (Gerhardt et al., 2003; Dorrell et al., 2002).

Because astrocytes are crucial for development of vascular patterning, disruption of astrocyte patterning in the retina severely disrupts vascular growth (Uemura et al., 2006). Under pathological conditions such as oxygen-induced retinopathy (OIR), astrocytes degenerate, leading to a breakdown of the blood retinal barrier (BRB) and pathological neovascularization (Stone et al., 1996). Rescue of astrocytes in OIR reduces this pathology (Dorrell et al., 2010). Here, we provide evidence that extracellular matrix components – laminins – guide astrocytes into the retina, promote at least one aspect of the maturation and regulate subsequent blood vessel development.

Laminins are key glycoprotein components of basement membranes (BMs), composed of three chains: α, β and γ (Yurchenco, 2011). Five α, three β and three γ chains have been identified forming 16 different heterotrimers (Aumailley et al., 2005; Macdonald et al., 2010) with overlapping yet distinct tissue distribution and function (Colognato and Yurchenco, 2000; Durbeej, 2010). The current nomenclature for laminins consists of three numbers, denoting the its chain composition, e.g. laminin-111 consists of α1, β1 and γ1 chains.

Laminins, containing the laminin β2 and γ3 chains, are expressed in retinal BMs, and are produced by neuroepithelial cells early in retinal development and by Müller glial cells in the mature retina (Libby et al., 1997; Libby et al., 2000). Moreover, deletion of laminin genes disrupts the formation of the retinal inner limiting membrane (ILM) (Pinzón-Duarte et al., 2010; Edwards et al., 2010). As laminins and their receptors regulate cell migration (Suh and Han, 2010; Fujiwara et al., 2004; Desban et al., 2006; Echtermeyer et al., 1996), including brain astrocytes *in vitro* (Armstrong et al., 1990), we hypothesize that laminins regulate both astrocyte migration and spatial organization in the retina.

To test this hypothesis, we examined astrocyte migration, patterning and subsequent blood vessel formation, in laminin mutant retinas. Our analyses demonstrate that β2- and γ3-containing laminins are indispensable for these processes *in vivo*. *In vitro* and *ex vivo* studies support the hypothesis that laminins regulate astrocyte migration in an isoform-specific manner. Furthermore,

Departments of Ophthalmology and Cell Biology, and the SUNY Eye Institute, State University of New York, Downstate Medical Center, 450 Clarkson Avenue, Brooklyn, New York 11203, USA.

*Author for correspondence (william.brunken@downstate.edu)

Accepted 3 March 2013

treatment with exogenous laminins rescues astrocyte migration and spatial patterning phenotype *ex vivo*. Together, these data support the hypothesis that β2- and γ3-containing laminins are important cues in retinal vascular development.

MATERIALS AND METHODS

Mice

Animal procedures were performed in accordance with the institutional committees. Targeted deletion of *Lamb2* and *Lamc3* genes and the production of the *Lamb2*$^{-/-}$*Lamc3*$^{-/-}$ animals have been described previously (Noakes et al., 1995; Li et al., 2012; Dénes et al., 2007; Pinzón-Duarte et al., 2010). The *Lamb2*- and *Lamc3*-null lines of animals were backcrossed over nine generations to C57bl/6J. The compound null line *Lamb2:c3* was maintained on a mixed genetic background of C57bl/6J and 129Sv/J; genetic background characterization was performed by Taconic (Germantown, NY) using a 377 SNP panel and demonstrated that the *Lamb2*$^{+/-}$*:Lamc3*$^{-/-}$ line matched over 83% of C57bl/6J recipient genome. The following notations are used for genotypes: β2 deletion, *Lamb2*-null or *Lamb2*$^{-/-}$; γ3 deletion, *Lamc3*-null or *Lamc3*$^{-/-}$; for compound deletion of β2 and γ3, *Lamb2;c3*-null or *Lamb2:c3*$^{-/-}$.

Retinal immunostaining

For whole-mount preparations, eyes were enucleated and fixed in 2% paraformaldehyde in PBS (PFA) for 10 minutes; the retinas were dissected and flat mounted and treated with absolute methanol at −20°C for 10 minutes. After washing in PBS, retinas were incubated overnight at 4°C in blocking buffer (15% goat or donkey serum; 0.03% Triton X-100; PBS). Next, sections were incubated with primary antibodies (in 5% goat or donkey serum; 0.01% Triton X-100; PBS) for 48 hours at 4°C, washed and incubated with secondary antibodies. Radial sections were prepared according to our previously published methods (Li et al., 2012; Pinzón-Duarte et al., 2010).

Reagents

Antibodies used were anti-laminin (Sigma, St Louis, MO, USA), β2 laminin (gift of Dr Sasaki, Max-Planck-Institut für Biochemie, Munich, Germany), γ3 laminin (R96, our laboratory), PDGFR-α (BD Biosciences, San Jose, CA, USA), rabbit anti-GFAP (Chemicon, Billerica, MA, USA), CD31 (Millipore, Billerica, MA, USA), Perlecan (Santa Cruz Biotechnology, Santa Cruz, CA, USA) and integrin β1 (Millipore). Goat anti-rabbit 488 and 568, goat anti-rat 488 and 568, donkey anti-rabbit 488 and 594, and donkey anti-rat 488 and 594 (Life Technologies, Grand Island, NY, USA) secondary antibodies were used. The specificity of the laminin antibodies has been published previously: anti-β2 (Pinzón-Duarte et al., 2010; Radner et al., 2013) and anti-γ3 antibodies (Li et al., 2012). The following laminins were used: EHS-laminin (Life Technologies), recombinant laminin-521 (BioLamina, Stockholm, Sweden) and laminin 5 (a gift from Dr Manuel Koch, Universität zu Köln, Germany). Additional reagents were low-melting agarose (Boston Bioproducts, Ashland, MA, USA), collagenase (cls 1) (Worthington Biochemical Corporation, Lakewood, NJ, USA) and papain (Sigma).

Measurements and statistics

Astrocyte migration and vascular growth were measured using Volocity (v 5.4.1, Perkin-Elmer, Waltham, MA, USA). Astrocyte migration and blood vessel growth measurements were made in all the quadrants and averaged. For tip cell quantification, the number of CD31-positive tip cells at the leading edges was marked and counted in a 150 μm^2 region in each quadrant. The mean value was calculated by averaging the number of tip cells in all four quadrants. To test for statistical significance of any differences, Student's *t*-test was performed and a *P* value of less than 0.05 was considered statistically significant.

Isolation of retinal astrocytes

Retinal astrocytes were isolated from P0-P3 wild-type and laminin nulls, as described previously (West et al., 2005), with modifications. In brief, retinas were treated with 1% collagenase type 1 (in DMEM, Life Technologies) for 30 minutes at 37°C and then treated with papain (0.5 mg/ml) at 37°C with 5% CO_2. The retinas were gently triturated in DMEM containing 10% FBS using pipette. The dissociated cells were spun and plated in 6-well culture plates (Corning Life Sciences, Tewksbury, MA). After 6 to 8 hours, the plates were shaken at regular intervals to remove other contaminating cells. The cells were grown for 12 days, detached using 0.25% trypsin and re-plated. The obtained cells were more than 90% astrocytes, judged by immunostaining for GFAP.

Agarose drop migration assay

The astrocyte migration assay was modified from published methods (Frost et al., 2000). Briefly, sterile coverslips were coated with PBS (control), laminin 332 (10 μg/ml) or EHS laminin (laminin 111, 10 μg/ml). The coated coverslips were placed in a 24-well chamber cell culture plate. Isolated wild-type astrocytes were trypsinized and suspended in a DMEM-low melting agarose mix (0.3% agarose: cell density: 2×10^6 cells per ml). Agarose-cell suspension (2 μl) was placed on the substrate-coated area, cooled at 4°C for 10 minutes. Then, 500 μl of standard media (DMEM, 10% heat-inactivated FBS) was added and the samples were incubated (37°C, 5% CO_2). Migration of astrocytes through the drop was scored every 6 hours. The experiment was stopped after 3 or 6 days by fixing the agarose drop for 5 minutes using 4% PFA and analyzed for GFAP expression. The presented data are from 6-day-old cultures. The numbers of GFAP-expressing astrocytes that migrated through the agarose and elaborated on the substrate-coated area were counted. This experiment was performed in duplicate and repeated.

Optic nerve head explant preparation

Eyes were enucleated with intact optic nerves from P7 wild-type animals. The optic nerve head (ONH) was dissected in sterile Hank's Balanced Salt Solution (HBSS; Sigma) and placed on a 0.4 μm transwell membrane insert; the bottom chamber was filled with standard medium and placed in an incubator. After 6 hours, the ONH was treated with exogenous laminin 332 (10 μg/ml), EHS laminin (10 μg/ml) or PBS (control) and maintained for 36 hours. The membrane with the ONH was fixed with 4% PFA for 5 minutes. The membrane was detached without disturbing the ONH. The ONH was blocked for 1 hour at room temperature and immunostaining was performed for GFAP as described above. This experiment was repeated using P10 and P14 wild-type ONH.

Integrin restoration and function blocking experiments

Astrocytes were isolated from P2 wild-type and Lamb2:c3-null retina. After trypsinization, single-cell suspensions were plated on prepared coverslips at low densities (100 to 250 cells) per coverslip and incubated. After 24 hours, the cells were fixed (4% PFA, 5 minutes), washed and immunostained for GFAP and β1 integrin. This experiment was performed in duplicate.

To block β1-integrin function, retinas were isolated from wild-type P0-P2 pups and the central region around the ONH was dissected. The explants were placed on EHS laminin (10-25 μg/ml) coverslips and cultured in standard medium. After 36 hours, one explant was incubated in medium with 10-25 μg/ml non-specific control IgG (Jackson ImmunoResearch Laboratory, West Grove, PA, USA) and the other in medium with 10-25 μg/ml integrin β1 antibody (BD Biosciences, San Jose, CA, USA). After 48 hours, the explants were fixed (4% PFA, 5 minutes), washed in PBS and blocked. The samples were further processed using our standard immunohistochemistry procedures.

Inner limiting membrane preparation

Inner limiting membranes (ILMs) were stripped according to published methods (Hu et al., 2010) with changes. Sterile coverslips were coated with 0.01% poly-D-lysine (PDL; Sigma). Retinas from P5-P15 animals were isolated in cold sterile PBS and spread on a sterile nitrocellulose paper, photoreceptor side facing the nitrocellulose paper. This preparation was placed on a PDL-coated coverslip with the vitreal surface of the retina on the coverslip. The nitrocellulose paper with attached retina was carefully peeled off the coverslip, leaving the ILM behind. The coverslips were incubated in 2% Triton X-100 at 4°C overnight to remove the cell debris; then were washed extensively in sterile distilled H_2O and then in PBS. To perform astrocyte migration assays, ONH explants (prepared as above) were placed on the stripped ILM and cultured under standard conditions for 2-3 days. Astrocyte migration was assayed GFAP IHC; the experiment was repeated on P7 and P3 explants.

Ex vivo rescue experiments

P0 or P1 Lamb2:c3-null retinas were dissected in sterile HBSS. Retina were flattened and placed photoreceptor side down on a Transwell membrane (0.4 μm, Corning). Medium was added to the bottom chamber until it contacted the membrane. The retinas were incubated overnight (37°C, 5% CO_2). The next day, either EHS-laminin (0.5 mg/ml) or laminin 521 + DMEM was added on top of one retina; the other received only additional DMEM. After 4 days, the organotypic retinal cultures were fixed (4% PFA, 10 minutes) and processed for GFAP immunohistochemistry.

Fluorescein angiography

Fluorescein angiographies were performed in P15 mice (n=3) as described previously (Lai et al., 2005). In brief, animals were anesthetized using intraperitoneal injection of ketamine (100 mg/kg body weight) and xylazine (10 mg/kg body weight), and the pupils were dilated with topical 1% tropicamide and 2.5% phenylephrine hydrochloride 10 minutes before imaging. A drop of hydroxypropyl methylcellulose demulcent solution (2.5%) was placed on each eye. The animals were then administered with 0.1 ml of 10% sodium fluorescein by intraperitoneal injection. Live recording was performed at different time scales using a Micron-II imaging system (Phoenix Research Laboratories, Pleasanton, CA, USA).

RESULTS

Deletion of *Lamb2* and *Lamc3* genes affects astrocyte migration and spatial patterning in the retina

At postnatal day (P) 15, the laminin β2 chain is expressed in Bruch's membrane, the ILM and retinal vascular basement membrane (BM) (Fig. 1A), with higher expression in arteries and microvasculature (Fig. 1B,C). The laminin γ3 chain is expressed in Bruch's membrane and the choroid plexus, and weakly in the ILM (Fig. 1D). In the vascular BM, γ3 laminin chain expression was restricted to only veins and microvessels (Fig. 1E,F). As astrocytes migrate over the retinal surface, we localized their migratory position relative to the laminin-rich ILM. Wild-type P0 retinal sections were co-labeled for laminin β2 chain (Fig. 1G) and for an early marker of astrocytes, PDGFRα (Fig. 1H). Astrocytes are wholly contained within the laminin β2-rich compartment, i.e. the ILM (Fig. 1I). We also examined whether astrocytes express the laminin receptor, integrin β1, which regulates brain astrocyte migration *in vitro* (Peng et al., 2008). We colocalized another marker of astrocytes, GFAP (Fig. 1J), with integrin β1 expression (Fig. 1K) at P0. GFAP-expressing astrocytes, migrating through the ILM, express the integrin β1 subunit (Fig. 1L).

We have previously shown that the ILM is somewhat disrupted in *Lamb2*-null animals and grossly disrupted in *Lamb2:c3*-null animals (Pinzón-Duarte et al., 2010). Astrocyte distribution at P15 is intact in both wild-type and *Lamc3*$^{-/-}$ animals, but in *Lamb2* and *Lamb2:c3* nulls, astrocytes are found only where the ILM is intact (supplementary material Fig. S1). Astrocyte migration takes place around birth from P0-P5; therefore, we examined retinae from control and each of the laminin mutants at P0, P1, P3 and P5 to examine the progress of migration *in situ*. In the second postnatal week, considerable remodeling of the astrocyte template occurs, so we examined retinae at P15 to determine the mature pattern.

GFAP, a marker for astrocytes, is expressed at low levels in astrocytes in the early (P0-P5) retina (West et al., 2005); PDGFRα was used as it better identifies astrocytes in early development. At P0, astrocytes in the wild-type retina had migrated over half of the retinal surface, advancing to 239.49±2.01 μm (all data are mean±s.e.m.) from the head of the optic nerve (Fig. 2A,E). Although the ILM remains morphologically intact in the *Lamc3*-null retina (supplementary material Fig. S1), the progress of

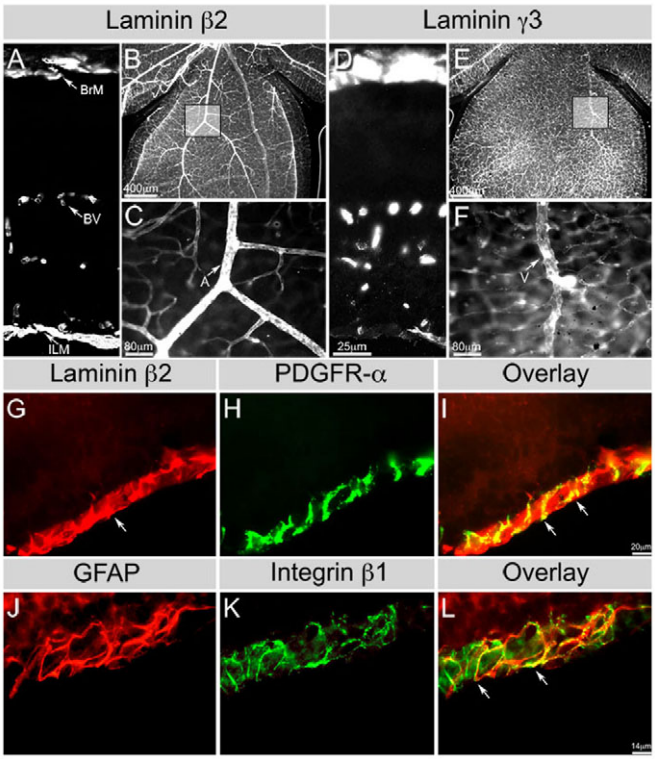

Fig. 1. Astrocytes migrate within β2-containing laminin-rich niche. (**A-C**) Laminin β2 distribution in the wild-type P15 retina (A, section; B,C, wholemount). Boxed area in B is shown in C. β2 chain is deposited in all retinal basement membranes (BMs). (**D-F**) Laminin γ3 distribution in the wild-type P15 retina (D, section; E,F, wholemount). Boxed area in E is shown in F. The γ3 chain is deposited most prominently in microvessel and venous BMs; some deposition is seen in the inner limiting membrane (ILM). Scale bar in D applies to A,D. BrM, Bruch's membrane; BV, blood vessels. (**G**,**H**) Wild-type P0 retinal section reacted with antibodies against laminin β2 chain (G) and PDGFRα (H). (**I**) Merge of G and H. Arrow in G indicates laminin β2 chain at the ILM. Arrows in I indicate PDGFRα-labeled astrocytes interacting with β2 chain-containing laminins at the ILM. (**J**,**K**) Wild-type P0 retinal section reacted with antibodies against GFAP (J) and β1 integrin (K) antibodies. (**L**) Merge of J and K. Arrows in L indicate β1 integrin in GFAP^{+} astrocytes.

astrocyte migration was significantly slowed from P0-P3 compared with controls (Fig. 2B,E). At P3, wild-type astrocytes migrated 345.97±5.23 μm, whereas *Lamc3*-null astrocytes covered only 257.86±5.86 μm (Fig. 2E). However, by P5, *Lamc3*-null astrocytes catch up to controls (Fig. 2E).

The progress of *Lamb2*-null astrocytes is significantly retarded throughout vascular development (Fig. 2C,E). At P0, *Lamb2*-null astrocytes migrated only 99.4±3.22 μm from the ONH; at P3, the astrocyte front extended to 176.72±9.31 μm. By P5, when the control astrocyte front has reached the retinal margin, it advanced to only 213.99±14.6 μm in the *Lamb2*-null animal. The combined deletion of *Lamb2* and *Lamc3* genes virtually halted astrocyte migration from the ONH (Fig. 2D). At P0, astrocytes in *Lamb2:c3*-null mouse migrated only 35.71±1.08 μm and advanced a mere 30 μm in the next 3 days, to 61.4±3.26 μm from the ONH. As in the *Lamb2* null, *Lamb2:c3*-null astrocytes did not reach the retinal periphery by P5. This migration is significantly delayed compared with controls.

By P15, wild-type astrocytes assumed their adult distribution, as did *Lamc3*-null astrocytes despite their initially slower migration

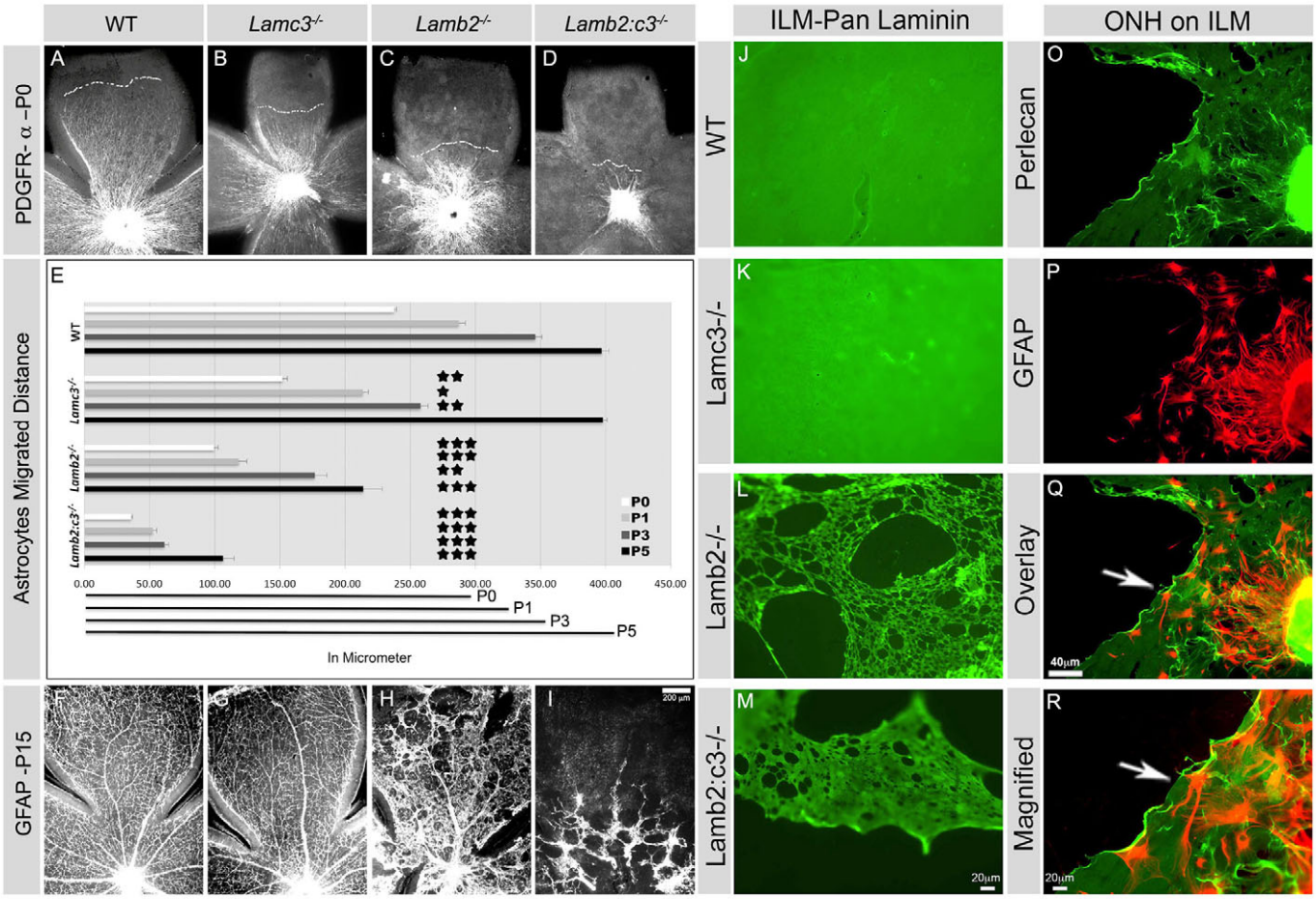

Fig. 2. Astrocyte migration and spatial organization is laminin dependent. (**A-D**) PDGFRα^{+} astrocyte distribution was analyzed at P0 in retinal wholemounts. The broken white lines mark the boundaries of astrocyte migration in each genotype. (**E**) Distances covered by astrocytes from P0 to P5. Average distance covered by astrocytes per quadrant of indicated genotypes (all are n=3 except Lamb2$^{-/-}$ P5, n=2). Error bars represent s.e.m. ***P≤0.001; **P≤0.003; *P≤0.01. The horizontal black lines at the bottom of the chart represent the average length of retinal quadrants from P0 to P5. (**F-I**) GFAP^{+} astrocyte distribution was analyzed in P15 retinal wholemounts. (**J-M**) The structure of the ILMs from P15 animals (genotype indicated) was studied using a pan-laminin antibody. Wild type and *Lamc3*$^{-/-}$ are uniform in appearance (J,K), whereas *Lamb2*$^{-/-}$ (L) and *Lamb2:c3*$^{-/-}$ (M) are defective with numerous large holes. (**N-P**) Wild-type ILM was used as a substrate for astrocyte (GFAP, red) migration from ONH explants. Wild-type P10 astrocytes (red) are seen spreading out over an stripped P10 ILM (perlecan green). (**Q**) The region indicated by the arrow in P at higher magnification. Scale bars: In I for A-D,F-I; in M for J-M; in Q for P,Q.

(Fig. 2F,G). By contrast, the distribution of *Lamb2*-null astrocytes was severely affected. In P15 *Lamb2* nulls, few astrocytes were present at the retinal periphery and their distribution was abnormal. In wholemounts, numerous regions of the retina were devoid of astrocytes (Fig. 2H), producing holes in the normal continuous sheet of astrocytes. Moreover, their classic star-like shape was lost; instead, the cells were fusiform. At P15, *Lamb2:c3*-null astrocytes were largely confined to central retina and were distributed in patches or cords of cells (Fig. 2I). In both *Lamb2* and *Lamb2:c3* nulls, astrocytes migrated abnormally over the surface of persistent hyaloid vessels. Together, these data strongly suggest that astrocyte migration and spatial patterning are dependent on laminin deposition in the ILM.

Astrocyte migration is laminin dependent and exogenous laminin restores migration in laminin nulls

We next tested whether the laminin-rich ILM niche induces astrocyte migration. We isolated ILM from P10-15 wild-type and laminin-null retina, and analyzed these for laminin expression. The ILM was isolated as an intact sheet with a homogenous deposition of laminin from both wild type and *Lamc3* null (Fig. 2J,K), whereas the ILM from *Lamb2* and *Lamb2:c3*-null retinae had a lattice-like appearance with large holes (Fig. 2L,M) (see also Hirrlinger et al., 2011).

To test the role of the ILM in astrocyte migration, we dissected the ONH from wild-type P10 mice, placed it on stripped wild-type ILM, cultured this for 2-3 days and examined astrocyte (GFAP+) migration on ILM (perlecan+). Astrocytes migrate robustly over the ILM (Fig. 2N-Q). Astrocytes preferred to stay within the ILM, suggesting that ILM is acting as a substrate for astrocyte migration.

We next used several migration assays to determine whether laminins act as haptotactic factors guiding astrocyte migration. Retinal astrocytes, isolated from wild-type P2 retinae, were suspended in an agarose drop placed on laminin-coated substrates. Astrocytes that elaborated processes on the coated substrates were quantified (Fig. 3A-D). On uncoated or laminin-332 (laminin

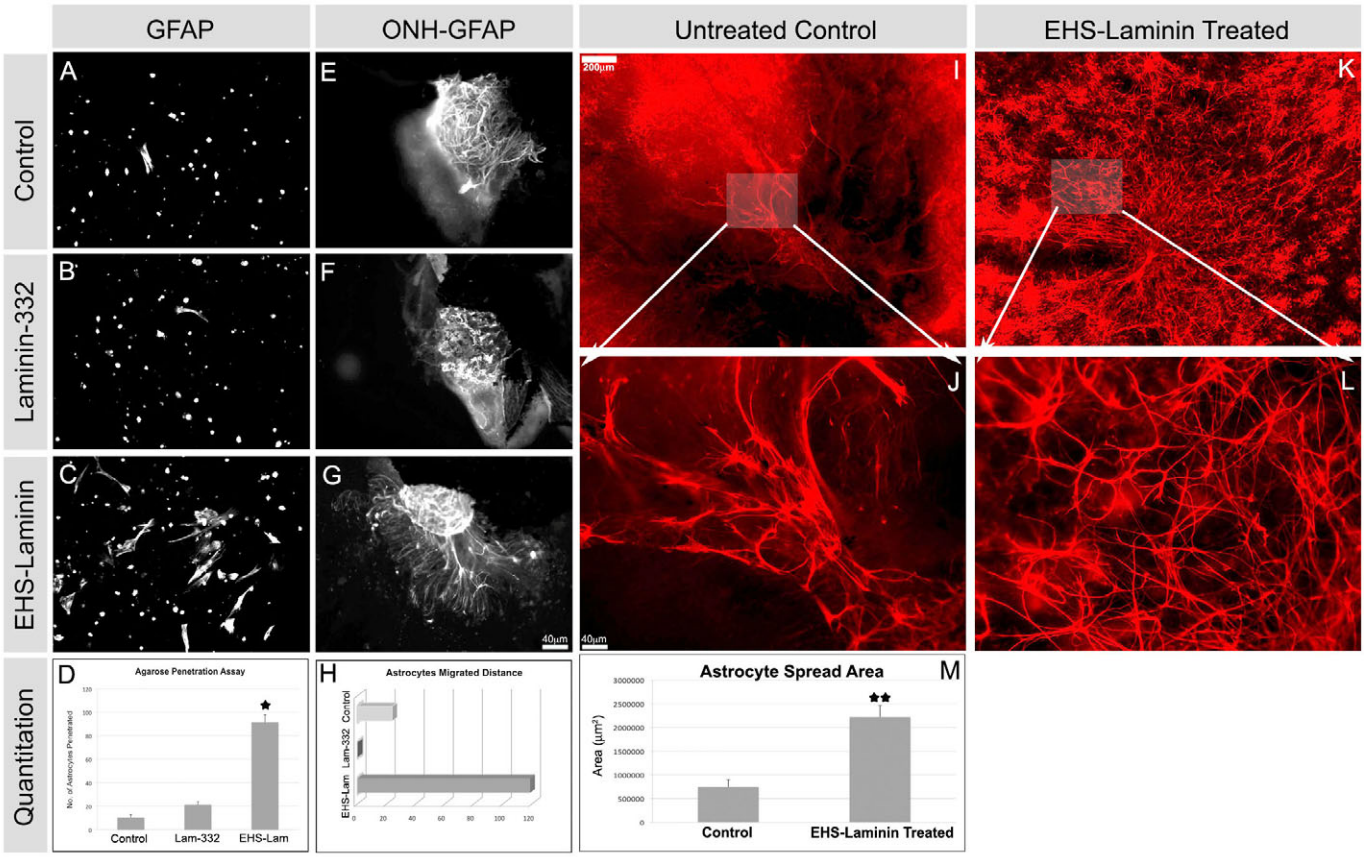

Fig. 3. Exogenous laminin promotes astrocyte migration and rescues the astrocyte-migration defect in laminin-null explants. (**A-D**) Migration of astrocytes (GFAP$^+$) from agarose suspension onto coverslips coated with indicated substrates was analyzed after 6 days. Cells in the suspension remained rounded; those penetrating the drop flatten onto the substrate (A-C). Astrocyte migration and spreading on EHS-laminin was significantly enhanced compared with other isoforms (D). Error bars indicate s.d. (*P<0.04). (**E-H**) The spread of astrocytes (GFAP$^+$) out of P7 ONH explants was enhanced by exogenous laminin in a isoform-specific manner. (H) The area covered by astrocytes that migrated from ONH explants were quantified; a single representative experiment is shown here. (**I-M**) Exogenous laminin (EHS-laminin) restores astrocyte migration in an organotypic culture of *Lamb2:c3*$^{-/-}$ retina. In untreated P1 retina, GFAP$^+$ astrocytes remain clustered around the ONH (arrow, I); they also maintain an immature spindle shape (J, magnified from I, as indicated). Addition of EHS-laminin restored astrocyte migration (K, arrow, ONH) and maturation of shape (L, magnified from K as indicated). (M) The area over which astrocytes spread was quantified and recorded. Error bars represent s.d. (**P<0.002). Scale bars: in I, 200 μm for I and K; 40 μm for J and L; in G, 40 μm for E-G.

α3β3γ2)-coated coverslips, few astrocytes penetrated the drop to the coverslip (Fig. 3A,B). By contrast, on EHS-laminin-coated coverslips, numerous astrocytes penetrated to the coverslip (Fig. 3C). There was an approximately fourfold increase in astrocyte penetration on EHS-laminin (Fig. 3D).

The previous assay used dissociated cells on an artificial surface, an admittedly artificial set of conditions. Thus, to further approximate the *in vivo* situation, we developed a second *ex vivo* explant culture. ONH explants from 1-week-old wild-type retinas were cultured on transwell membrane either untreated or with exogenous laminin. There was little astrocyte migration out of the untreated control or laminin-332-treated ONH explants (Fig. 3E-H), whereas EHS-laminin treatment induced robust migration (Fig. 3G,H). These data demonstrate that laminins induce astrocyte migration in an isoform-specific manner (Fig. 3D,H).

In vivo rescue of the laminin defect with intraocular injection is impractical because laminins have limited diffusion. As an alternative we treated mutant retinae in organotypic culture with exogenous laminins. For this experiment, we chose *Lamb2:c3*-null retina, because the combined null has the most severe defects (Fig. 2). Organotypic cultures were prepared from P0 or P1 *Lamb2:c3* nulls and were treated for 4 days with exogenous EHS-laminin *ex vivo*.

We chose EHS-laminin (laminin 111) because it had the most robust activity in our *in vitro* and *ex vivo* migration assays (above). In untreated *Lamb2:c3*-null retinal cultures, GFAP-expressing astrocytes were present mostly clumped around the ONH (Fig. 3I,J), consistent with our observations of *Lamb2:c3*-null retinas *in vivo*. Strikingly, exogenous addition of EHS-laminin to the *Lamb2:c3*-null retinal culture significantly restored astrocyte migration and patterning [Fig. 3K,L; 3M, control (n=4) and treated (n=5) P<0.002].

We next tested whether the addition of laminin-521, a laminin composed of the predominant laminin chains found in the native ILM (Balasubramani et al., 2010) would restore astrocyte behavior. In untreated controls, astrocytes were clumped together and did not have their normal morphology (supplementary material Fig. S2A,B). Exogenous laminin-521 restored astrocyte migration and spatial organization in *Lamb2*-null retinal organotypic cultures (supplementary material Fig. S2C,D). These *ex vivo* experiments

demonstrate that laminins are key for astrocyte migration and patterning in the retina.

Loss of laminin affects β1 integrin expression specifically in astrocytes

As noted above, β1 integrins are expressed by astrocytes in the laminin-rich ILM (Fig. 1); these integrins are necessary for brain astrocyte migration *in vitro* (Peng et al., 2008). Thus, we asked whether the ablation of laminins affects β1 integrin expression. We localized β1 integrin and GFAP in P5 wild-type and laminin-null retinas. In wild-type and *Lamc3*-null P5 retinas, β1 integrin colocalized with GFAP in astrocytes (Fig. 4A-F). By contrast, deletion of *Lamb2* alone or with *Lamc3* markedly affected β1 integrin expression specifically in astrocytes (Fig. 4G-L). In these nulls, β1 integrin immunoreactivity was completely absent in the GFAP+ astrocytes (Fig. 4G-L). We calculated the Pearson coefficient for colocalization of the GFAP and β1 integrin (Fig. 4). Importantly, β1 integrin continued to be expressed in endothelial cells (Fig. 4). The experiment was repeated three times in whole-mount retinae with similar results, as well as in radial sections. Together, these data suggest that the deletion of laminin substrates affects integrin receptor localization in astrocytes.

To test whether this downregulation of integrin expression is a direct consequence of the loss of an interaction with extracellular laminins, we isolated astrocytes from wild-type and *Lamb2:c3*-null P2 retinas, and analyzed β1 integrin expression in the presence or absence of exogenous laminins after 24 hours in culture. In the absence of exogenous laminins, isolated wild-type astrocytes secrete and deposit laminin-111 as well as laminin β2 (supplementary material Fig. S3), whereas neither *Lamb2*-null nor *Lamb2:c3*-null astrocytes secrete and deposit laminin-111 (supplementary material Fig. S3). In the absence of exogenous laminins, wild-type retinal astrocytes formed a few processes, with β1 integrin localized at the process extensions (Fig. 5A-C), suggesting that these cells produced a matrix and were adhering to it. By contrast, *Lamb2:c3*-null astrocytes plated on uncoated coverslips were small and rounded with few, if any, processes or integrin β1 expression (Fig. 5D-F). Wild-type retinal astrocytes cultured on EHS-laminin-coated coverslips produced abundant processes, with integrin localization at well-organized focal adhesion points (Fig. 5G-I) in which FAK and ILK are expressed (not shown). In contrast to their behavior on uncoated glass, *Lamb2:c3*-null retinal astrocytes grown on EHS laminin-coated coverslips behaved identically to wild type astrocytes and extended numerous processes with β1 integrin localized at the focal adhesion points (Fig. 5J-L).

We then asked whether the interaction of integrin β1 receptor with laminins is required for astrocyte migration. Wild-type P0 retinas containing the ONH were dissected and placed on EHS-laminin coated coverslips. After 36-48 hours of culture, astrocytes migrated out of the explant. At this time, the explants were treated with either control or integrin β1 IgG. Control IgG treatment did not affect astrocyte migration and they migrated 205.4±20.9 μm from the explant (Fig. 5M,Q). The astrocytes showed elongated process formation over the laminin-coated surface (Fig. 5N). Integrin β1 antibody treatment reduced astrocyte migration as they migrated only 24.6±7.5 μm from the explant (Fig. 5O,Q). The integrin antibody also reduced process elongation and cytoskeletal organization, resulting in a rounded cell appearance (Fig. 5Q).

Laminin deletion affects retinal vascular growth

Retinal vascular growth is dependent on astrocyte migration and patterning (Schnitzer, 1988; Uemura et al., 2006); thus, we analyzed whether vascular growth was also affected in laminin-null retinas. Retinas of P1, P3, P5 and P15 from wild type and laminin nulls were analyzed for vascular growth with an endothelial specific marker, CD31. Blood vessel formation in the wild-type retinas covered 306.47±9.03 μm at P5 (Fig. 6A,E). By contrast, in the *Lamc3*-null retinas, the growth of blood vessel formation was significantly delayed (P<0.001) and covered 223.14±11.85 μm at P5 (Fig. 6B,E). Because vascular growth was delayed in *Lamc3*-

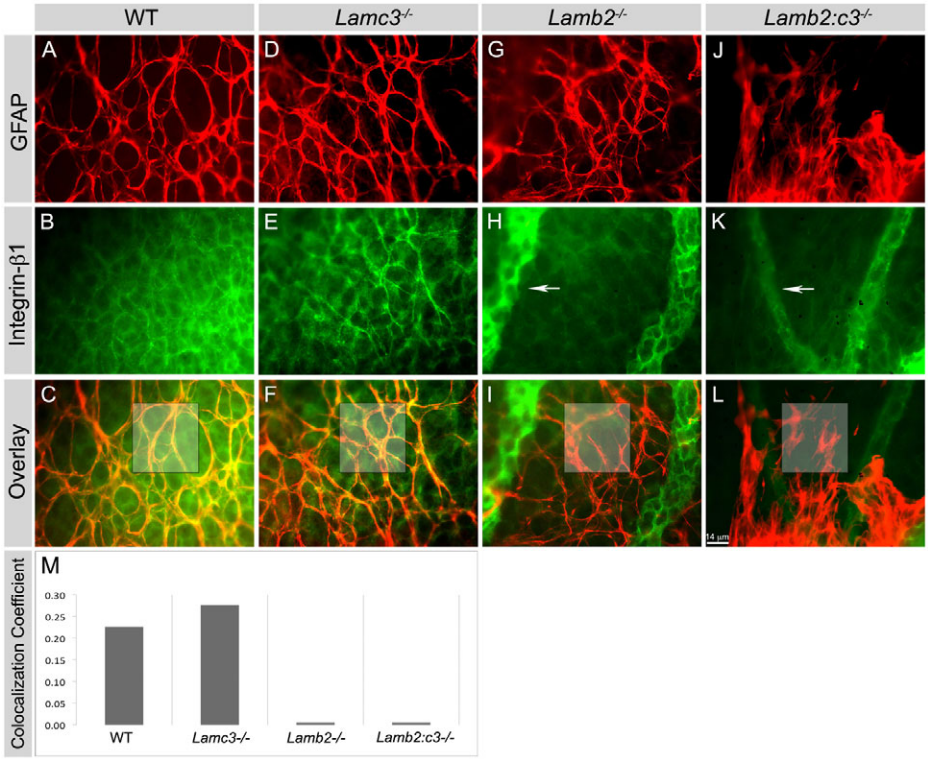

Fig. 4. Deletion of laminins affects expression of β1 integrin in astrocytes *in vivo*. (**A-L**) The expression of integrin β1 was studied in P5 retinal wholemounts. GFAP$^+$ astrocytes (red) express integrin β1 (green) in both wild-type and *Lamc3*$^{-/-}$ (yellow, C and F) retina but not in the *Lamb2* mutants (I and L). Integrin β1 expression in endothelial cells (GFAP$^-$ cells) in all genotypes, particularly in the persistent hyaloid vessels (arrows, H and K). (**M**) Pearson's colocalization coefficient was calculated for the boxed areas in images C-L. Scale bar: 14 μm.

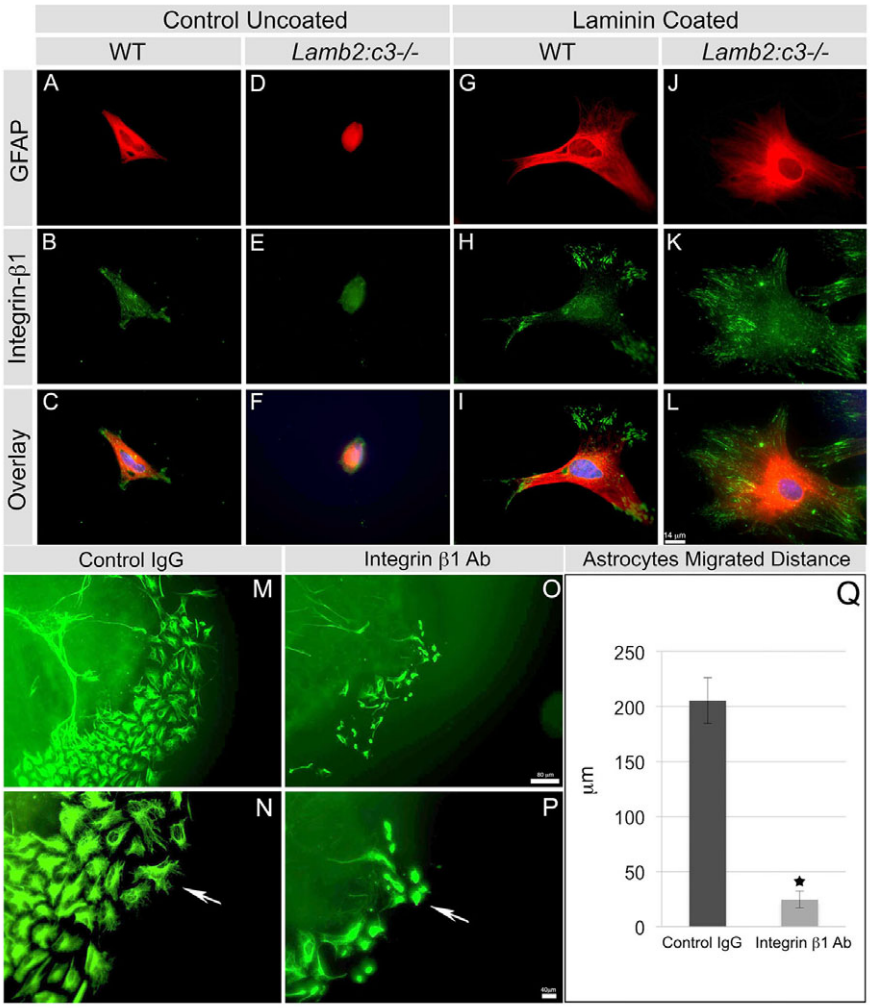

Fig. 5. Exogenous laminin restores focal localization of β1 integrin in laminin-null astrocytes. (**A-F**) The astrocyte structure from P2 wild-type (A-C) and mutant (D-F) retinas were analyzed after 24 hours of culture with the indicated markers. DAPI (blue) labels the nucleus in the overlays. (**G-L**) EHS-laminin-coated substrates enhanced the spread of P2 wild-type (G-I) and mutant (J-L) astrocytes. (**M-P**) Function-blocking antibodies against integrin β1 prevent astrocyte migration from ONH explants. Explants were grown on EHS-laminin substrates in the presence of control IgG (M,N) or integrin β1 antibody (O,P) for 48 hours. EHS-laminin induced robust astrocyte (GFAP^{+}) migration in the control treatment (M) and migrating cells showed elongated filopodia (arrow, N). Treatment with integrin β1 antibody reduced astrocyte migration (O) and filopodial elongation (P). Scale bars: 14 μm in A-L; 80 μm in M,O; 40 μm in N,P. (**Q**) Quantification of distance that astrocytes migrated away from the explants. Error bars represent s.e.m. *P<0.01.

null retinas, we determined whether the tip cell number was altered at the leading edge of the expanding vasculature. At P5, we found that the number of tip cells in the *Lamc3*-null retina was significantly reduced (P<0.001) compared with wild type (Fig. 6J; supplementary material Fig. S4C,D).

In the γ3-null retina, the advancing vascular front is more heavily branched (compare Fig. 6A,B and supplementary material Fig. S4E,F). To understand further whether the laminin γ3 chain regulates vascular branching, we colocalized CD31 and the laminin γ3 chain in wild-type P5 retinas and found that the laminin γ3 chain was predominantly deposited at the notches of the growing vascular branches (supplementary material Fig. S4A,B). As microglia regulate endothelial cell anastomosis through Notch signaling (Outtz et al., 2011), we also determined whether the normal distribution of these cells was altered. Indeed, more microglia were recruited to vascular branch points in the *Lamc3*-null than control (supplementary material Fig. S5E,F). Because microglia are associated with vascular branching, this increased recruitment of microglia may lead to increased vascular branching. By P15, blood vessel growth and patterning appeared normal in the *Lamc3*-null retina (Fig. 6G), consistent with astrocyte migration recovery (above).

In the *Lamb2*-null retina, the few endothelial sprouts that entered the retina were unable to migrate further, even at P5 (Fig. 6C,E). By P15, blood vessel formation was incomplete in the *Lamb2*-null animal. The surface capillary network was entirely absent in the most peripheral regions of the retina (Fig. 6H) and surviving hyaloid vessels were obvious. In the *Lamb2:c3*-null retina, vascular growth was severely affected at all stages (Fig. 6D,E,I). At P5, there is no endothelial wave front visible and only the loose networks of adherent hyaloid vessels are obvious. By P15, a small network of microvessels had formed in the central most regions of the retina. Persistent hyaloid vessels were present, and in most cases they sprouted into the retina. Such persistent vessels are reminiscent of those in individuals with Pearson syndrome, a disease that results from mutations in the human laminin β2 gene *LAMB2* (see Discussion).

Laminins are crucial for maintaining proper astrocyte-endothelial interaction and vascular integrity

We next tested whether astrocyte-endothelial interactions, as well as permeability, were affected in the retinas in the absence of laminins. In wild-type and *Lamc3*-null retinas at P15, astrocytes were spatially organized and the processes of astrocytes neatly wrapped around the blood vessels (Fig. 7A,B). However, in P15 *Lamb2*-null and *Lamb2:c3*-null retinas, the spatial organization of astrocytes was compromised: astrocytes clumped over the vascular BM and did not wrap around the blood vessels, as in the wild type (Fig. 7C,D).

Fluorescein angiography was used to detect signs of vascular leakage in laminin-null mice. In wild-type and *Lamc3*-null retinas, there was no vascular leakage, and the fluorescein dye was well retained within the blood vessels (120 seconds after dye injection

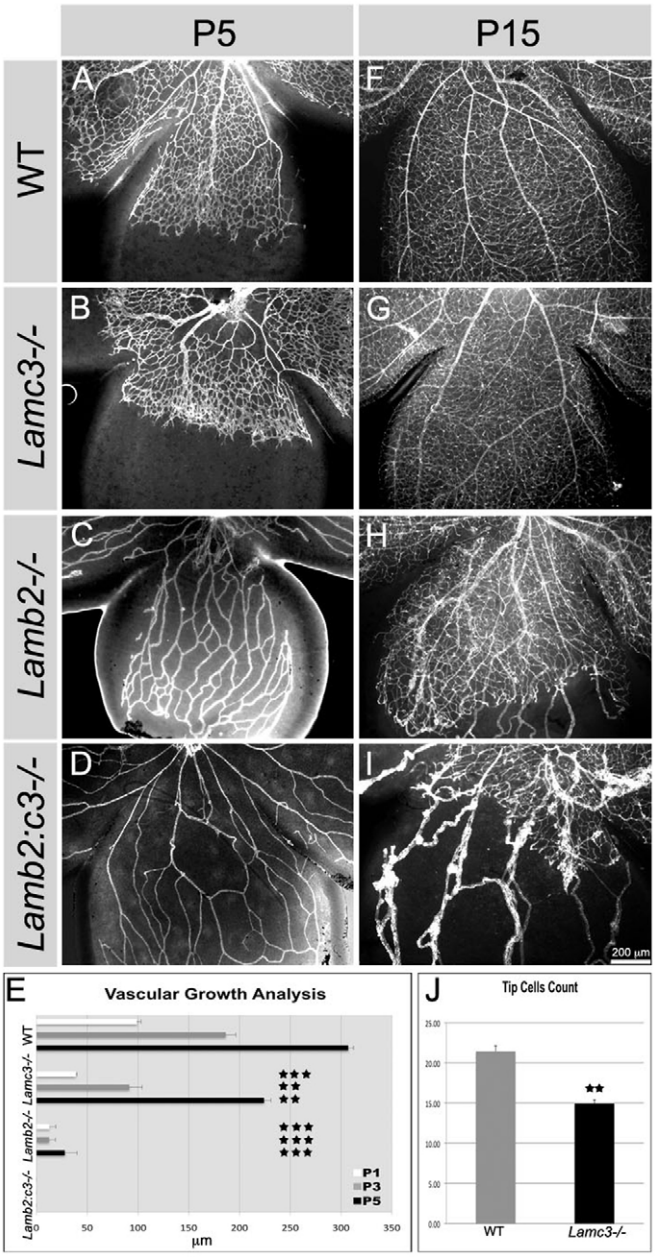

Fig. 6. Deletion of laminins retards vascular growth. (**A-D**) Vascular growth was assayed by CD31 expression at P5 in retinal wholemounts. (**E**) Vascular growth was charted for the indicated ages and genotypes (n=3 or 4). Error bars represent s.e.m. No outgrowth of endothelial cells were seen in the *Lamb2:c3*$^{-/-}$ mice from P1 to P5. (**F-I**) Vascular growth assayed at P15 from indicated genotypes. Vascular growth recovers by P15 in the Lamc3$^{-/-}$ (G) but not the other Lamb2 mutants; vessels in I are persistent hyaloid vessels. (**J**) Tip cells were counted in a 150 µm^2 region in each quadrant of the P5 retina (n=4). Error bars represent s.d. ***P≤0.0002, **P≤0.001.

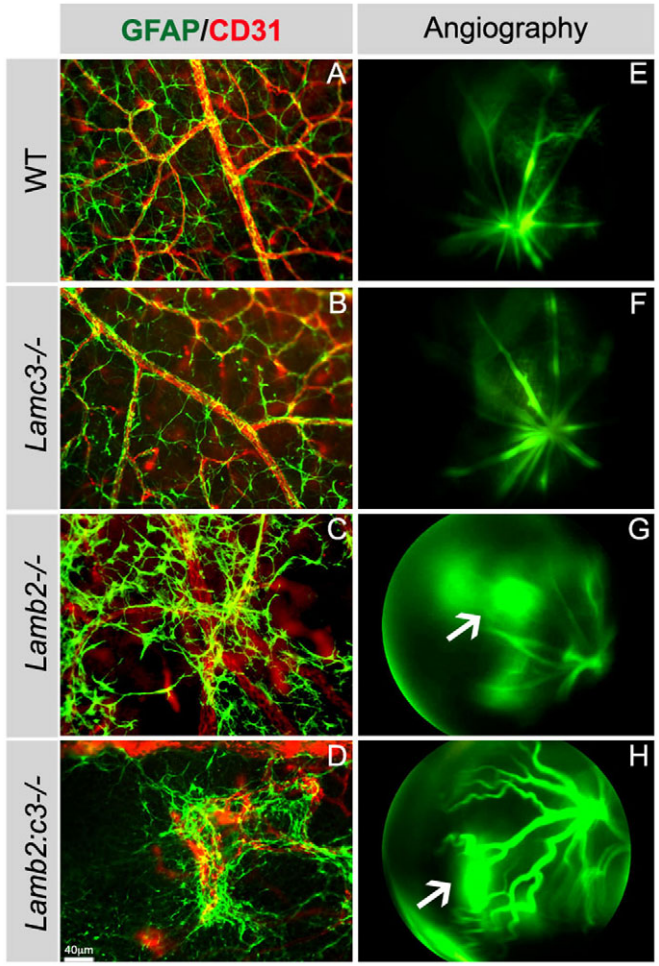

Fig. 7. Deletion of laminins affects vascular integrity. (**A-D**) The interaction between astrocytes (GFAP$^+$) and endothelial cells (CD31$^+$) was examined in P15 retinas from the indicated genotypes. (**E-H**) Vascular integrity was examined with fluorescein angiography; a time point 120 seconds after dye injection is shown from P15 animals. Arrows in G and H indicate vascular leakage.

shown in Fig. 7E,F). By contrast, severe vascular leakage was observed in the *Lamb2*-null and *Lamb2:c3*-null retinas throughout the observation period (120 seconds after injection shown in Fig. 7G,H, arrows). These studies demonstrate that laminins containing the β2 and γ3 chains are crucial for maintaining astrocyte-endothelial interactions and the stability of the vascular wall.

DISCUSSION

Astrocyte migration and patterning is regulated by laminins present in the ILM

An astrocyte-derived template is crucial for the development of retinal angiogenesis (Dorrell et al., 2002; Uemura et al., 2006). In adults, astrocytes play a crucial role in maintaining the blood-retinal barrier (BRB). To date, the factors that guide astrocytes into the retina are not well characterized. However, astrocytes isolated from the rat brain migrate towards laminin (Armstrong et al., 1990), suggesting a possible role for laminins in inducing astrocyte migration. In this study, using both *in vivo* and *in vitro* assays, we provide evidence that laminins at the ILM regulate astrocyte migration, spatial organization and subsequent vascular growth.

In the retina, laminins are crucial for ILM formation (Pinzón-Duarte et al., 2010; Hirrlinger et al., 2011; Halfter et al., 2005; Edwards et al., 2010). Similarly, mutations in α-dystroglycan (a laminin receptor) and in an enzyme that participates in glycosylation of α-dystroglycan (POMGnT1) also produce defective deposition of laminin at the ILM, resulting in defective ILM formation (Lee et al., 2005; Takahashi et al., 2011). In addition to ILM disruption,

laminin, dystroglycan and POMGnT1 mutants also display abnormal astrocyte distribution and blood vessel formation (Edwards et al., 2010; Lee et al., 2005; Takahashi et al., 2011). These studies demonstrate that an intact ILM is necessary for normal astrocyte distribution in the retina. Here, we show that deletion of *Lamb2* and *Lamb2:c3* genes results in defective ILM assembly with large holes (Fig. 2). Most likely this is because the laminin β2 chain is the predominant β subunit in the ILM (Balasubramani et al., 2010), and other laminin β subunits fail to compensate for its loss in the *Lamb2* and *Lamb2:c3* mutants.

Although the deletion of the laminin γ3 chain did not severely affect astrocyte patterning, its deletion did reduce the rate of migration at early postnatal days. This suggests that the laminin γ3 chain may regulate astrocyte-ILM interactions during migration. This is consistent with the observation that the presence of the γ3 chain in a laminin inhibits integrin binding (Ido et al., 2008) and may alter the balance between adhesion and migration.

Our *in vivo* analysis of laminin nulls suggests that particular laminins in the ILM may act as haptotactic factors and guide astrocytes over the retinal surface. The combined deletion of β2 and γ3 chains produced a severe defect in astrocyte migration and patterning. In *Lamb2:c3* nulls, astrocytes were not only defectively distributed, they also fasciculated and formed a net-like pattern rather than tiling over the surface of the retina. Our *in vitro* and ONH explant migration assays clearly demonstrate that astrocytes prefer to migrate on EHS-laminin (laminin 111)-coated substrates compared with laminin-332-coated or uncoated substrates.

In addition, treatment of *Lamb2* and *Lamb2:c3*-null retinal cultures with EHS-laminin or laminin 521 rescued astrocyte migration and their spatial patterning (Fig. 3; supplementary material Fig. S2). These data demonstrate that, in addition to providing a substrate for migration, specific laminins help astrocytes to attain their spatial positioning.

The laminin α1, α5, β2 and γ1 chains are the predominant laminin subunits present in the ILM (Balasubramani et al., 2010); thus, the dominant laminins in the ILM are likely to be 121 and 521. The treatment of *Lamb2 and Lamb2:c3*-null retinal cultures with EHS-laminin (containing mostly laminin 111) or laminin 521 provided physiologically relevant ligands for integrin expression and activation regulating migration and spatial positioning. However, it is also possible that exogenous laminin treatment may have restored the expression of some other factors, either soluble or fixed, that regulate astrocyte migration and patterning. Just one example is PDGFA (Fruttiger et al., 1996); further experiments are needed to assess how these factors are affected by laminin deletion. Nevertheless, our data clearly demonstrate that laminins are indispensable for astrocyte migration and patterning in the retina, although it is not known whether it is because they provide direct cues to astrocytes or are vital to the structural and biological integrity of the ILM.

Laminins are required for integrin expression in astrocytes

Some of the key steps that take place during cell migration during development are polarization, cytoskeletal reorientation and lamellipodial extension (Ridley et al., 2003; Huttenlocher, 2005). These events are mediated, in part, by the interaction of extracellular matrix molecules, including laminins, with integrins. For example, in keratinocytes, laminin-integrin interactions result in keratinocyte polarization, lamellipodia extension and induction of migration (Choma et al., 2007). Similarly, laminin-integrin interactions regulate embryonic stem cell migration (Suh and Han, 2010).

Laminin-integrin interactions also affect astrocytes. Activation of integrins during astrocyte migration results in astrocyte polarization and process extension (Etienne-Manneville and Hall, 2001). Conversely, inhibition of integrins in astrocytes affects polarization and process extension (Etienne-Manneville and Hall, 2001). Integrin β1-null astrocytes in culture also demonstrate defects in polarization, process extension and abnormal migration (Peng et al., 2008).

Previous *in vitro* culture models have shown that cells deposit laminins and use them as substrates on which to polarize and migrate (Frank and Carter, 2004). Astrocytes isolated from *Lamb2* and *Lamb2:c3*-null retinas demonstrate defective laminin secretion in culture (supplementary material Fig. S3). When *Lamb2:c3*-null astrocytes were grown on glass coverslips for 24 hours, most cells failed to extend processes and were unable to localize integrin β1, which could be due to the lack of laminin secretion. However, when *Lamb2:c3*-null astrocytes were grown on EHS-laminin, they rapidly induced numerous process extensions, with focal localization of integrin β1. These results demonstrate that laminins are crucial for focal localization of integrins, which in turn is necessary for cell adhesion and migration.

Functional blocking of integrin β1 receptor not only affects astrocyte migration, it also affects filopodia-like process extension in the presence of laminin (Fig. 5). These data indicate that laminin-integrin β1 interactions are necessary for laminin-directed astrocyte migration. It will be interesting to further investigate the downstream signaling events that were disrupted in laminin-null astrocytes during migration.

Laminins are necessary for retinal vascular development

Endothelial tip cells follow a template laid down by astrocytes in the retina (Gerhardt et al., 2003; Dorrell et al., 2002). Disruption of astrocyte template formation affects vascular growth progression (Uemura et al., 2006), supporting the importance of astrocytes during retinal vascular development. It is possible that astrocytes make a laminin-rich matrix, which provides a substrate for endothelial cell migration. A recent study has shown a laminin-integrin α6β1 interaction in endothelial tip cell selection (Estrach et al., 2011). Here, we show that the deletion of laminin chains has differential effects on endothelial migration over an astrocyte template. Analysis of *Lamc3*-null retinas showed slower vascular growth progression at early postnatal days. The effect could be due to the delay in astrocyte patterning. However, in these *Lamc3* nulls, we observed increased vascular branching at the leading edges of the growing vasculature and a concomitant increase in microglial recruitment to the branch points at the vascular front (supplementary material Fig. S5). These results, coupled with the selective location of γ3 to the branch points, suggest that laminins containing γ3 negatively regulate the recruitment of microglia at the vascular branch points to prevent excessive branching during retinal vascular development. Indeed mice lacking microglia have reduced vascular branching (Rymo et al., 2011).

In both *Lamb2* and *Lamb2:c3* nulls, vascular growth was severely affected in both early and late postnatal days. This effect could be due to a lack of proper astrocyte template formation. Astrocytes isolated from *Lamb2*- and *Lamb2:c3*-null retinas fail to secrete laminin (supplementary material Fig. S3). This result suggests that the lack of astrocyte-derived laminin in $Lamb2^{-/-}$ and $Lamb2:c3^{-/-}$ retinas disrupts endothelial migration. Similarly, defective vascular growth was observed in *Lama1* mutant retinas (Edwards et al. 2010). It is possible that astrocyte-derived α1- and

β2-containing laminins are regulating endothelial migration in the CNS.

In addition to defective vascular growth, we observed persistent hyaloid vessels (HVs) in both *Lamb2*- and *Lamb2:c3*-null retinae. Persistence of the HVs is common when retinal vascular development is disrupted either in animal models (Edwards et al., 2010) or in human diseases such as retinopathy of prematurity and familial exudative vitreoretinopathy (FEVR) (Nissenkorn et al., 1988; Errais et al., 2008). The trigger for vessel regression itself is not well understood but the most likely explanation is hemodynamics. The retinal vessels and HVs are organized in parallel. As flow through the retinal limb increases, flow in the HV limb will decrease and thereby trigger regression (Ribatti and Crivellato, 2012). The normal regression of HVs is mediated by macrophage lineage cells (Lee et al., 2009). A defect in macrophage recruitment in *Lamb2:c3*-null animals during HV regression requires further investigation.

Our analyses clearly show that laminins containing the β2 and γ3 chains play important and distinctive roles during development. With regard to the β2 chain, individuals with Pierson syndrome have multiple ocular defects, including persistent fetal vasculature (Pierson et al., 1963). Pierson syndrome has been shown to be a consequence of mutations in *LAMB2*, and a multigenerational mennonite family with Pierson syndrome and mutations in *LAMB2* has both chorioretinal pigmentary changes and abnormal retinal vascular development (Mohney et al., 2011). Other individuals with mutations in *LAMB2* and Pierson syndrome exhibit retinal vascular defects (Bredrup et al., 2008). Recent reports also suggest a possibility of the role of various genetic mutations in other diseases, such as familial exudative vitreoretinopathy and retinopathy of prematurity (Dickinson et al., 2006). It will be worthwhile verifying the possibilities of mutations in laminin genes in proliferative retinopathies in order to better understand the pathology in these diseases.

Laminins maintain vascular stability

Loss of laminin-binding integrin and dystroglycan receptors at the astrocyte-vascular interface occurs in models of ischemia (Wagner et al., 1997; Tagaya et al., 2001; Milner et al., 2008). Astrocytes play a crucial role in maintaining the blood-brain barrier (Abbott et al., 2006), and astrocytes can induce properties of the blood-brain barrier in cultured endothelial cells (Wolburg et al., 1994; Gardner et al., 1997). These data suggest that laminins mediate astrocyte and endothelial interactions, thereby maintaining vascular stability. We have not extensively analyzed the effect of laminin deletion on pericyte distribution. Preliminary data suggest that they are abnormal but these data need further expansion. As these mural cells are vitally important to vascular integrity, further investigations into their structure and function should be undertaken.

The interaction of astrocytes with the vascular BM is abnormal in *Lamb2*- and *Lamb2:c3*-null retinas. Most astrocytes in these retinas clumped abnormally over the vascular BM, wrapping around the vascular wall. Abnormal interaction of astrocytes with the vascular BM in these retinas may have resulted in vascular leakage. It is possible that the loss of laminins may affect receptor localization at the astrocyte-vascular BM interface, and it will be interesting to analyze the *Lamb2*- and *Lamb2:c3*-null retinas for the distribution of laminin receptors that are expressed at the astrocyte-vascular BM interface, such as integrins containing α6, α1 and β4 subunits, and dystroglycan. Our *in vivo* analyses indicate that the laminin β2 and γ3 chains are necessary for astrocyte-endothelial interactions and the maintenance of vascular integrity.

In conclusion, our *in vivo* and *in vitro* studies demonstrate that laminins are indispensable for astrocyte migration and subsequent blood vessel formation in the retina. Deletion of the laminin β2 and γ3 chains disrupts astrocyte migration, spatial patterning and subsequent blood vessel formation in the retina.

Acknowledgements
The authors thank our colleague Dr Willi Halfter (University of Pittsburgh) for teaching us the technique of ILM stripping.

Funding
This work was supported by grants from the National Institutes of Health [R01 EY012676; U54 HD071594 to W.J.B.]; and unrestricted funds from Research to Prevent Blindness, Inc. to the Department of Ophthalmology. Deposited in PMC for release after 12 months.

Competing interests statement
The authors declare no competing financial interests.

Supplementary material
Supplementary material available online at
http://dev.biologists.org/lookup/suppl/doi:10.1242/dev.087817/-/DC1

References

Abbott, N. J., Rönnbäck, L. and Hansson, E. (2006). Astrocyte-endothelial interactions at the blood-brain barrier. *Nat. Rev. Neurosci.* **7**, 41-53.
Armstrong, R. C., Harvath, L. and Dubois-Dalcq, M. E. (1990). Type 1 astrocytes and oligodendrocyte-type 2 astrocyte glial progenitors migrate toward distinct molecules. *J. Neurosci. Res.* **27**, 400-407.
Aumailley, M., Bruckner-Tuderman, L., Carter, W. G., Deutzmann, R., Edgar, D., Ekblom, P., Engel, J., Engvall, E., Hohenester, E., Jones, J. C. et al. (2005). A simplified laminin nomenclature. *Matrix Biol.* **24**, 326-332.
Balasubramani, M., Schreiber, E. M., Candiello, J., Balasubramani, G. K., Kurtz, J. and Halfter, W. (2010). Molecular interactions in the retinal basement membrane system: a proteomic approach. *Matrix Biol.* **29**, 471-483.
Bredrup, C., Matejas, V., Barrow, M., Bláhová, K., Bockenhauer, D., Fowler, D. J., Gregson, R. M., Maruniak-Chudek, I., Medeira, A., Mendonça, E. L. et al. (2008). Ophthalmological aspects of Pierson syndrome. *Am. J. Ophthalmol.* **146**, 602-611.
Chen, J. and Smith, L. E. (2007). Retinopathy of prematurity. *Angiogenesis* **10**, 133-140.
Choma, D. P., Milano, V., Pumiglia, K. M. and DiPersio, C. M. (2007). Integrin alpha3beta1-dependent activation of FAK/Src regulates Rac1-mediated keratinocyte polarization on laminin-5. *J. Invest. Dermatol.* **127**, 31-40.
Colognato, H. and Yurchenco, P. D. (2000). Form and function: the laminin family of heterotrimers. *Dev. Dyn.* **218**, 213-234.
Dénes, V., Witkovsky, P., Koch, M., Hunter, D. D., Pinzón-Duarte, G. and Brunken, W. J. (2007). Laminin deficits induce alterations in the development of dopaminergic neurons in the mouse retina. *Vis. Neurosci.* **24**, 549-562.
Desban, N., Lissitzky, J. C., Rousselle, P. and Duband, J. L. (2006). alpha1beta1-integrin engagement to distinct laminin-1 domains orchestrates spreading, migration and survival of neural crest cells through independent signaling pathways. *J. Cell Sci.* **119**, 3206-3218.
Dickinson, J. L., Sale, M. M., Passmore, A., FitzGerald, L. M., Wheatley, C. M., Burdon, K. P., Craig, J. E., Tengtrisorn, S., Carden, S. M., Maclean, H. et al. (2006). Mutations in the NDP gene: contribution to Norrie disease, familial exudative vitreoretinopathy and retinopathy of prematurity. *Clin. Experiment. Ophthalmol.* **34**, 682-688.
Dorrell, M. I., Aguilar, E. and Friedlander, M. (2002). Retinal vascular development is mediated by endothelial filopodia, a preexisting astrocytic template and specific R-cadherin adhesion. *Invest. Ophthalmol. Vis. Sci.* **43**, 3500-3510.
Dorrell, M. I., Aguilar, E., Jacobson, R., Trauger, S. A., Friedlander, J., Siuzdak, G. and Friedlander, M. (2010). Maintaining retinal astrocytes normalizes revascularization and prevents vascular pathology associated with oxygen-induced retinopathy. *Glia* **58**, 43-54.
Durbeej, M. (2010). Laminins. *Cell Tissue Res.* **339**, 259-268.
Echtermeyer, F., Schöber, S., Pöschl, E., von der Mark, H. and von der Mark, K. (1996). Specific induction of cell motility on laminin by alpha 7 integrin. *J. Biol. Chem.* **271**, 2071-2075.
Edwards, M. M., Mammadova-Bach, E., Alpy, F., Klein, A., Hicks, W. L., Roux, M., Simon-Assmann, P., Smith, R. S., Orend, G., Wu, J. et al. (2010). Mutations in Lama1 disrupt retinal vascular development and inner limiting membrane formation. *J. Biol. Chem.* **285**, 7697-7711.
Errais, K., Ammous, I., Kamoun, R., Mili Boussen, I., Anene, R., Zhioua, R. and Meddeb Ouertani, A. (2008). [Familial exudative vitreoretinopathy associated with persistence of hyaloid artery]. *J. Fr. Ophtalmol.* **31**, e3.

Estrach, S., Cailleteau, L., Franco, C. A., Gerhardt, H., Stefani, C., Lemichez, E., Gagnoux-Palacios, L., Meneguzzi, G. and Mettouchi, A. (2011). Laminin-binding integrins induce Dll4 expression and Notch signaling in endothelial cells. *Circ. Res.* **109**, 172-182.
Etienne-Manneville, S. and Hall, A. (2001). Integrin-mediated activation of Cdc42 controls cell polarity in migrating astrocytes through PKCzeta. *Cell* **106**, 489-498.
Frank, D. E. and Carter, W. G. (2004). Laminin 5 deposition regulates keratinocyte polarization and persistent migration. *J. Cell Sci.* **117**, 1351-1363.
Frost, E. E., Milner, R. and Ffrench-Constant, C. (2000). Migration assays for oligodendrocyte precursor cells. *Methods Mol. Biol.* **139**, 265-278.
Fruttiger, M. (2007). Development of the retinal vasculature. *Angiogenesis* **10**, 77-88.
Fruttiger, M., Calver, A. R., Krüger, W. H., Mudhar, H. S., Michalovich, D., Takakura, N., Nishikawa, S. and Richardson, W. D. (1996). PDGF mediates a neuron-astrocyte interaction in the developing retina. *Neuron* **17**, 1117-1131.
Fruttiger, M., Calver, A. R. and Richardson, W. D. (2000). Platelet-derived growth factor is constitutively secreted from neuronal cell bodies but not from axons. *Curr. Biol.* **10**, 1283-1286.
Fujiwara, H., Gu, J. and Sekiguchi, K. (2004). Rac regulates integrin-mediated endothelial cell adhesion and migration on laminin-8. *Exp. Cell Res.* **292**, 67-77.
Gardner, T. W., Lieth, E., Khin, S. A., Barber, A. J., Bonsall, D. J., Lesher, T., Rice, K. and Brennan, W. A., Jr (1997). Astrocytes increase barrier properties and ZO-1 expression in retinal vascular endothelial cells. *Invest. Ophthalmol. Vis. Sci.* **38**, 2423-2427.
Gerhardt, H., Golding, M., Fruttiger, M., Ruhrberg, C., Lundkvist, A., Abramsson, A., Jeltsch, M., Mitchell, C., Alitalo, K., Shima, D. et al. (2003). VEGF guides angiogenic sprouting utilizing endothelial tip cell filopodia. *J. Cell Biol.* **161**, 1163-1177.
Halfter, W., Willem, M. and Mayer, U. (2005). Basement membrane-dependent survival of retinal ganglion cells. *Invest. Ophthalmol. Vis. Sci.* **46**, 1000-1009.
Hirrlinger, P. G., Pannicke, T., Winkler, U., Claudepierre, T., Varshney, S., Schulze, C., Reichenbach, A., Brunken, W. J. and Hirrlinger, J. (2011). Genetic deletion of laminin isoforms β2 and γ3 induces a reduction in Kir4.1 and aquaporin-4 expression and function in the retina. *PLoS ONE* **6**, e16106.
Hu, H., Candiello, J., Zhang, P., Ball, S. L., Cameron, D. A. and Halfter, W. (2010). Retinal ectopias and mechanically weakened basement membrane in a mouse model of muscle-eye-brain (MEB) disease congenital muscular dystrophy. *Mol. Vis.* **16**, 1415-1428.
Huttenlocher, A. (2005). Cell polarization mechanisms during directed cell migration. *Nat. Cell Biol.* **7**, 336-337.
Ido, H., Ito, S., Taniguchi, Y., Hayashi, M., Sato-Nishiuchi, R., Sanzen, N., Hayashi, Y., Futaki, S. and Sekiguchi, K. (2008). Laminin isoforms containing the γ3 chain are unable to bind to integrins due to the absence of the glutamic acid residue conserved in the C-terminal regions of the γ1 and γ2 chains. *J. Biol. Chem.* **283**, 28149-28157.
Kempen, J. H., O'Colmain, B. J., Leske, M. C., Haffner, S. M., Klein, R., Moss, S. E., Taylor, H. R., Hamman, R. F. and the Eye Diseases Prevalence Research Group (2004). The prevalence of diabetic retinopathy among adults in the United States. *Arch. Ophthalmol.* **122**, 552-563.
Lai, C. M., Shen, W. Y., Brankov, M., Lai, Y. K., Barnett, N. L., Lee, S. Y., Yeo, I. Y., Mathur, R., Ho, J. E., Pineda, P. et al. (2005). Long-term evaluation of AAV-mediated sFlt-1 gene therapy for ocular neovascularization in mice and monkeys. *Mol. Ther.* **12**, 659-668.
Lee, Y., Kameya, S., Cox, G. A., Hsu, J., Hicks, W., Maddatu, T. P., Smith, R. S., Naggert, J. K., Peachey, N. S. and Nishina, P. M. (2005). Ocular abnormalities in Large(myd) and Large(vls) mice, spontaneous models for muscle, eye, and brain diseases. *Mol. Cell. Neurosci.* **30**, 160-172.
Lee, H. J., Ahn, B. J., Shin, M. W., Jeong, J. W., Kim, J. H. and Kim, K. W. (2009). Ninjurin1 mediates macrophage-induced programmed cell death during early ocular development. *Cell Death Differ.* **16**, 1395-1407.
Li, Y. N., Radner, S., French, M. M., Pinzón-Duarte, G., Daly, G. H., Burgeson, R. E., Koch, M. and Brunken, W. J. (2012). The γ3 chain of laminin is widely but differentially expressed in murine basement membranes: expression and functional studies. *Matrix Biol.* **31**, 120-134.
Libby, R. T., Xu, Y., Selfors, L. M., Brunken, W. J. and Hunter, D. D. (1997). Identification of the cellular source of laminin β2 in the adult and developing vertebrate retina. *J. Comp. Neurol.* **389**, 655-667.
Libby, R. T., Champliaud, M. F., Claudepierre, T., Xu, Y., Gibbons, E. P., Koch, M., Burgeson, R. E., Hunter, D. D. and Brunken, W. J. (2000). Laminin expression in adult and developing retinae: evidence of two novel CNS laminins. *J. Neurosci.* **20**, 6517-6528.
Macdonald, P. R., Lustig, A., Steinmetz, M. O. and Kammerer, R. A. (2010). Laminin chain assembly is regulated by specific coiled-coil interactions. *J. Struct. Biol.* **170**, 398-405.
Milner, R., Hung, S., Wang, X., Spatz, M. and del Zoppo, G. J. (2008). The rapid decrease in astrocyte-associated dystroglycan expression by focal cerebral ischemia is protease-dependent. *J. Cereb. Blood Flow Metab.* **28**, 812-823.
Mohney, B. G., Pulido, J. S., Lindor, N. M., Hogan, M. C., Consugar, M. B., Peters, J., Pankratz, V. S., Nasr, S. H., Smith, S. J., Gloor, J. et al. (2011). A novel mutation of LAMB2 in a multigenerational mennonite family reveals a new phenotypic variant of Pierson syndrome. *Ophthalmology* **118**, 1137-1144.
Nissenkorn, I., Kremer, I. and Ben-Sira, I. (1988). Association of a persistent hyaloid artery and ROP. *Ophthalmology* **95**, 559-560.
Noakes, P. G., Gautam, M., Mudd, J., Sanes, J. R. and Merlie, J. P. (1995). Aberrant differentiation of neuromuscular junctions in mice lacking s-laminin/laminin beta 2. *Nature* **374**, 258-262.
Outtz, H. H., Tattersall, I. W., Kofler, N. M., Steinbach, N. and Kitajewski, J. (2011). Notch1 controls macrophage recruitment and Notch signaling is activated at sites of endothelial cell anastomosis during retinal angiogenesis in mice. *Blood* **118**, 3436-3439.
Peng, H., Shah, W., Holland, P. and Carbonetto, S. (2008). Integrins and dystroglycan regulate astrocyte wound healing: the integrin beta1 subunit is necessary for process extension and orienting the microtubular network. *Dev. Neurobiol.* **68**, 559-574.
Pierson, M., Cordier, J., Hervouet, F. and Rauber, G. (1963). Une curieuse association malformative congenitale et familiale atteignant l'oeil et le rein. (An unusual congenital and familial congenital malformative combination involving the eye and kidney.). *J. Genet. Hum.* **12**, 184-213.
Pinzón-Duarte, G., Daly, G., Li, Y. N., Koch, M. and Brunken, W. J. (2010). Defective formation of the inner limiting membrane in laminin beta2- and gamma3-null mice produces retinal dysplasia. *Invest. Ophthalmol. Vis. Sci.* **51**, 1773-1782.
Provis, J. M. and Hendrickson, A. E. (2008). The foveal avascular region of developing human retina. *Arch. Ophthalmol.* **126**, 507-511.
Provis, J. M., Sandercoe, T. and Hendrickson, A. E. (2000). Astrocytes and blood vessels define the foveal rim during primate retinal development. *Invest. Ophthalmol. Vis. Sci.* **41**, 2827-2836.
Radner, S., Banos, C., Bachay, G., Li, Y. N., Hunter, D. D., Brunken, W. J. and Yee, K. T. (2013). β2 and γ3 laminins are critical cortical basement membrane components: Ablation of Lamb2 and Lamc3 genes disrupts cortical lamination and produces dysplasia. *Dev. Neurobiol.* **73**, 209-229.
Ribatti, D. and Crivellato, E. (2012). 'Sprouting angiogenesis', a reappraisal. *Dev. Biol.* **372**, 157-165.
Ridley, A. J., Schwartz, M. A., Burridge, K., Firtel, R. A., Ginsberg, M. H., Borisy, G., Parsons, J. T. and Horwitz, A. R. (2003). Cell migration: integrating signals from front to back. *Science* **302**, 1704-1709.
Rymo, S. F., Gerhardt, H., Wolfhagen Sand, F., Lang, R., Uv, A. and Betsholtz, C. (2011). A two-way communication between microglial cells and angiogenic sprouts regulates angiogenesis in aortic ring cultures. *PLoS ONE* **6**, e15846.
Sapieha, P., Hamel, D., Shao, Z., Rivera, J. C., Zaniolo, K., Joyal, J. S. and Chemtob, S. (2010). Proliferative retinopathies: angiogenesis that blinds. *Int. J. Biochem. Cell Biol.* **42**, 5-12.
Schnitzer, J. (1988). Astrocytes in mammalian retina. *Prog. Retin. Eye Res.* **7**, 209-231.
Stone, J., Chan-Ling, T., Pe'er, J., Itin, A., Gnessin, H. and Keshet, E. (1996). Roles of vascular endothelial growth factor and astrocyte degeneration in the genesis of retinopathy of prematurity. *Invest. Ophthalmol. Vis. Sci.* **37**, 290-299.
Suh, H. N. and Han, H. J. (2010). Laminin regulates mouse embryonic stem cell migration: involvement of Epac1/Rap1 and Rac1/cdc42. *Am. J. Physiol. Cell Physiol.* **298**, C1159-C1169.
Tagaya, M., Haring, H. P., Stuiver, I., Wagner, S., Abumiya, T., Lucero, J., Lee, P., Copeland, B. R., Seiffert, D. and del Zoppo, G. J. (2001). Rapid loss of microvascular integrin expression during focal brain ischemia reflects neuron injury. *J. Cereb. Blood Flow Metab.* **21**, 835-846.
Takahashi, H., Kanesaki, H., Igarashi, T., Kameya, S., Yamaki, K., Mizota, A., Kudo, A., Miyagoe-Suzuki, Y., Takeda, S. and Takahashi, H. (2011). Reactive gliosis of astrocytes and Müller glial cells in retina of POMGnT1-deficient mice. *Mol. Cell. Neurosci.* **47**, 119-130.
Uemura, A., Kusuhara, S., Wiegand, S. J., Yu, R. T. and Nishikawa, S. (2006). Tlx acts as a proangiogenic switch by regulating extracellular assembly of fibronectin matrices in retinal astrocytes. *J. Clin. Invest.* **116**, 369-377.
Wagner, S., Tagaya, M., Koziol, J. A., Quaranta, V. and del Zoppo, G. J. (1997). Rapid disruption of an astrocyte interaction with the extracellular matrix mediated by integrin alpha 6 beta 4 during focal cerebral ischemia/reperfusion. *Stroke* **28**, 858-865.
Watanabe, T. and Raff, M. C. (1988). Retinal astrocytes are immigrants from the optic nerve. *Nature* **332**, 834-837.
West, H., Richardson, W. D. and Fruttiger, M. (2005). Stabilization of the retinal vascular network by reciprocal feedback between blood vessels and astrocytes. *Development* **132**, 1855-1862.
Wolburg, H., Neuhaus, J., Kniesel, U., Krauss, B., Schmid, E. M., Ocalan, M., Farrell, C. and Risau, W. (1994). Modulation of tight junction structure in blood-brain barrier endothelial cells. Effects of tissue culture, second messengers and cocultured astrocytes. *J. Cell Sci.* **107**, 1347-1357.
Yurchenco, P. D. (2011). Basement membranes: cell scaffoldings and signaling platforms. *Cold Spring Harb. Perspect. Biol.* **3**, a004911.

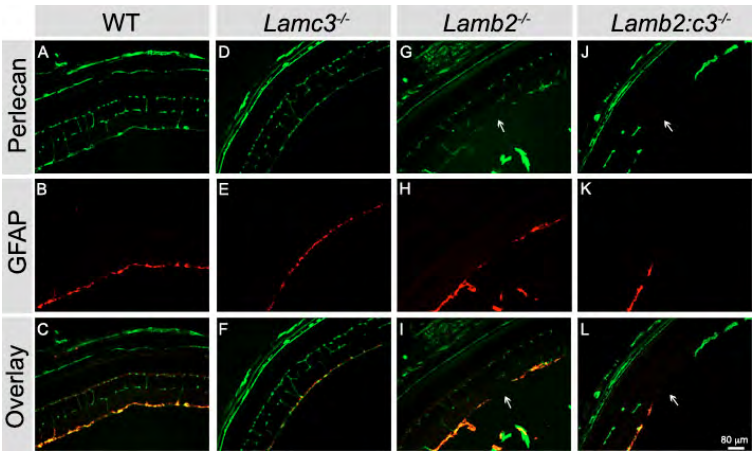

Fig. S1. Astrocytes are present only in retinal regions where the ILM is relatively intact. (**A-C**) Wild-type P15 retinal sections were reacted with antibodies to perlecan, a component of basement membranes (A), and GFAP, which is expressed by astrocytes (B). (C) Overlay of A and B. (**D-F**) *Lamc3*$^{-/-}$ P15 retinal sections were reacted with antibodies to perlecan (D) and GFAP (E). (F) Overlay of D and E. (**G-I**) *Lamb2*$^{-/-}$ P15 retinal sections were reacted with antibodies to perlecan (G) and GFAP (H). (I) Overlay of G and H. The ILM is disrupted in the *Lamb2*$^{-/-}$ retinal section (arrows). (**J-L**) *Lamb2:c3*$^{-/-}$ P15 retinal sections were reacted with antibodies to perlecan (J) and GFAP (K). (L) Overlay of J and K. The ILM is severely disrupted in the *Lamb2:c3*$^{-/-}$ retinal section (arrow).

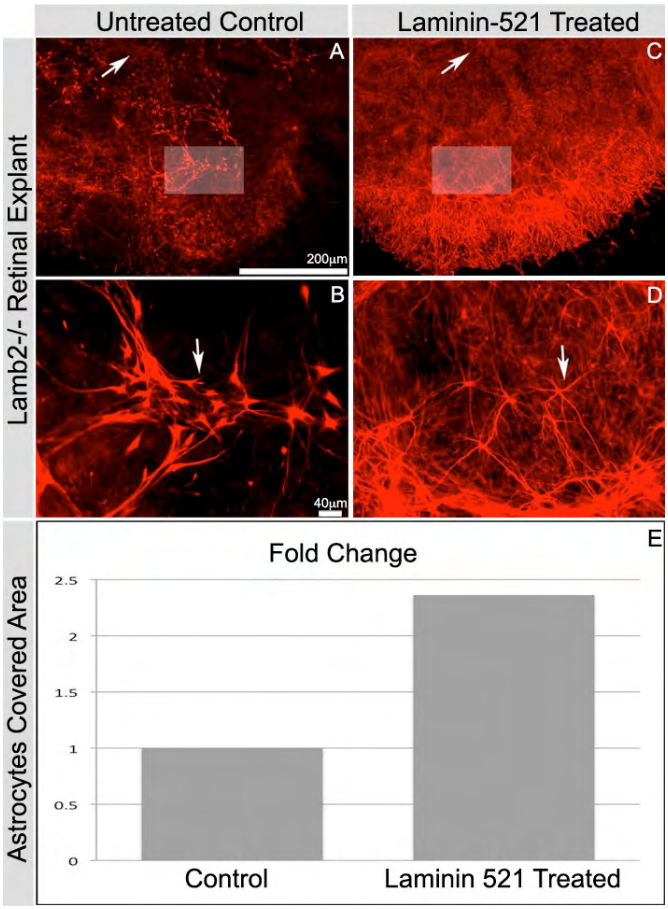

Fig. S2. Exogenous addition of laminin 521 restores astrocyte migration and patterning. (**A**,**B**) Untreated P1 *Lamb2*$^{-/-}$ retinal explants grown for 10 days in culture and analyzed for GFAP expression. Arrow indicates the head of the optic nerve. (B) A magnified region of A, indicated in by the shaded box in A. GFAP-positive astrocytes are clumped together (arrow in B). (**C**) Laminin 521-treated P1 *Lamb2*$^{-/-}$ retinal explant grown for 10 days in culture and analyzed for GFAP expression. Arrow indicates the head of the optic nerve. (**D**) A magnified region of C indicated by the shaded box in C. GFAP-positive astrocytes attain a stellate morphology with the addition of laminin 521 (arrow). (**E**) The difference in area covered by astrocytes between A and C was determined using Volocity software (v. 5.4.1) and the fold difference was recorded. This experiment was repeated using P0 and P3 *Lamb2*-null retinal cultures. Scale bar: 200 µm in A,C; 40 µm in B,D.

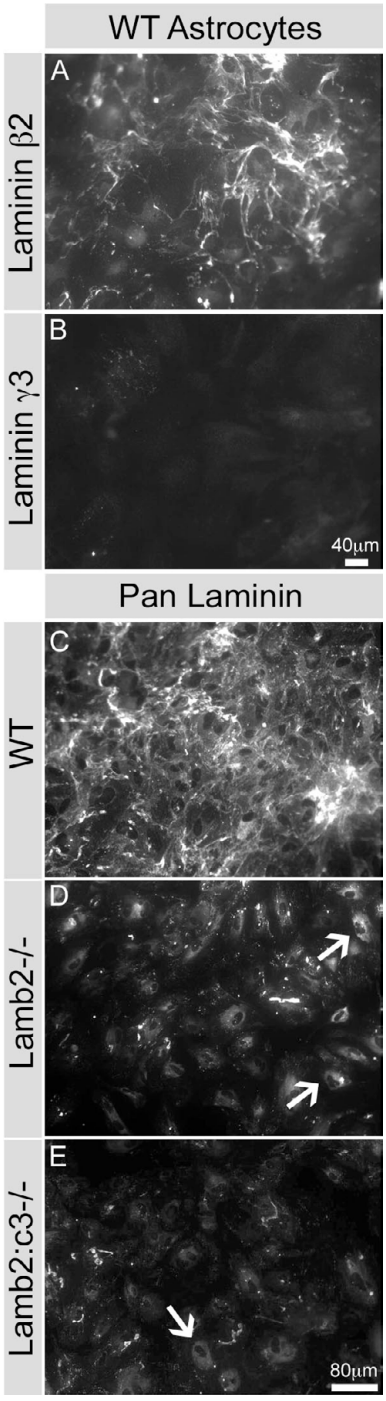

Fig. S3. Deletion of *Lamb2* and *Lamb2:c3* genes affects laminin secretion. (**A**) Wild-type retinal astrocytes were analyzed for laminin β2 chain expression after 6 days of culture. (**B**) Wild-type retinal astrocytes were analyzed for laminin γ3 chain expression after 6 days of culture. (**C**) Wild-type retinal astrocytes were analyzed for pan-laminin expression after 6 days of culture. (**D**) Lamb2$^{-/-}$ retinal astrocytes were analyzed for pan-laminin expression after 6 days in culture. Laminin immunoreactivity is mostly intracellular (arrows). (**E**) *Lamb2:c3*$^{-/-}$ retinal astrocytes were analyzed for pan-laminin expression after 6 days in culture. Laminin immunoreactivity is mostly intracellular (arrows). Scale bar: 40 μm in A,B; 80 μm in C,E.

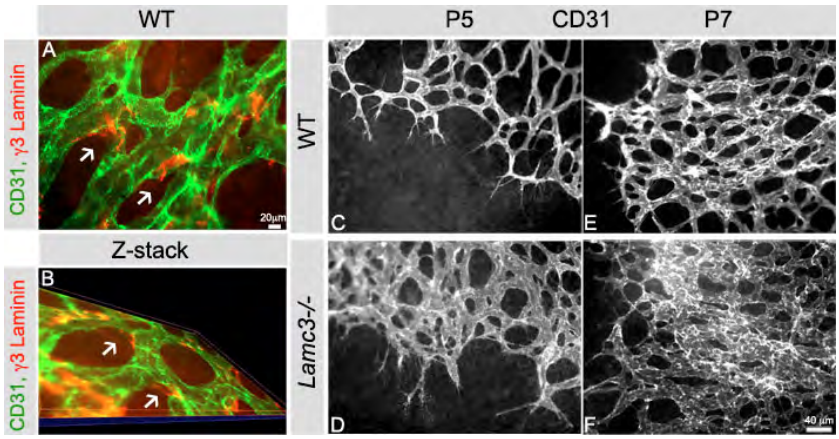

Fig. S4. Deletion of laminin γ3 chain affects vascular branching pattern during angiogenesis. (**A**) Wild-type P5 whole-mount retina was reacted with antibodies to laminin γ3 chain (red) and CD31 (green). The laminin γ3 chain is prominent at vascular branch points (arrows). This image was captured using fluorescent microscopy and de-convolved using Volocity. Scale bar: 20 μm. (**B**) Wild-type P5 whole-mount retina was reacted with antibodies to laminin γ3 chain (red) and CD31 (green). A *z*-stack was created from 0.5 μm steps using Volocity software (v. 5.4.1) and a three-dimensional image was created in Volocity and rotated to reveal the expression laminin γ3 chain around the vascular branch points (arrows). (**C**,**E**) Wild-type P5 and P7 whole-mount retinas were reacted with antibodies to CD31 to analyze the vascular branching pattern and tip cells at the vascular front. A regular branching array was observed in the wild-type retina. (**D**,**F**) *Lamc3*$^{-/-}$ P5 and P7 whole-mount retinas were reacted with antibodies to CD31 to analyze the vascular branching pattern and tip cells at the vascular front. The branching array is disrupted in the absence of the laminin γ3 chain. Scale bar: in F, 40 μm for C-F.

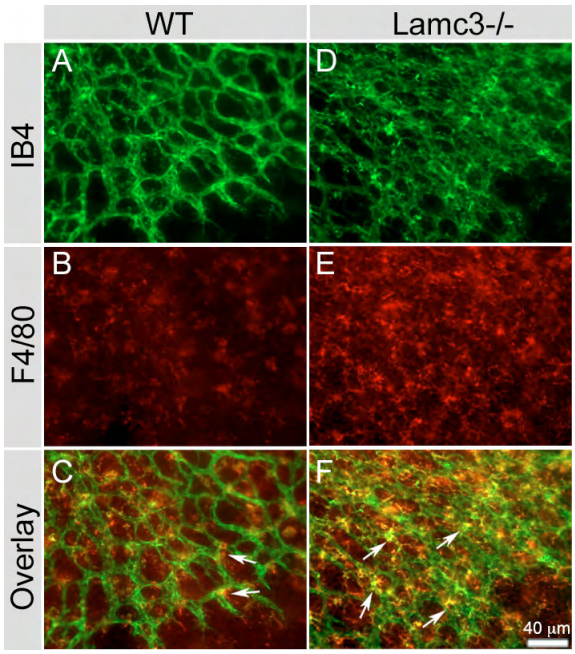

Fig. S5. Laminin γ3 chain regulates microglia-vasculature interactions. P3 whole-mount retinae from wild-type and *Lamc3*$^{-/-}$ were analyzed with isolection B4 (IB4, green) and F4/80 (a microglia-specific marker, red) to reveal blood vessel and microglia interactions. (**A**,**D**) Isolectin B4 demonstrates blood vessels as well as microglia in green. (**B**,**E**) F4/80 demonstrates only microglia in red. (**C**) Overlay of A and B demonstrates a few microglia at the vascular branch points (represented by arrows). (**F**) Overlay of D and E demonstrates more microglial associations with blood vessels at branch points (represented by arrows).